Phase and TV Based Convex Sets for Blind Deconvolution of Microscopic Images

Mohammad Tofighi[1], Onur Yorulmaz[1], Kıvanç Köse[2], Rengül Çetin-Atalay[3], and A. Enis Çetin, *Fellow, IEEE*[1]

[1]Department of Electrical and Electronics Engineering, Bilkent University, Ankara, Turkey,
[2]Dermatology Service, Memorial Sloan Kettering Cancer Center, New York, NY, USA,
[3]Bioinformatics Department, Graduate School of Informatics, Middle East Technical University, Ankara, Turkey.

***Abstract*—In this article, two closed and convex sets for blind deconvolution problem are proposed. Most blurring functions in microscopy are symmetric with respect to the origin. Therefore, they do not modify the phase of the Fourier transform (FT) of the original image. As a result blurred image and the original image have the same FT phase. Therefore, the set of images with a prescribed FT phase can be used as a constraint set in blind deconvolution problems. Another convex set that can be used during the image reconstruction process is the Epigraph Set of Total Variation (ESTV) function. This set does not need a prescribed upper bound on the total variation of the image. The upper bound is automatically adjusted according to the current image of the restoration process. Both the TV of the image and the point spread function are regularized using the ESTV set. Both the phase information set and the ESTV are closed and convex sets. Therefore they can be used as a part of any blind deconvolution algorithm. Simulation examples are presented.**

***Index Terms*—Projection onto Convex Sets, Blind Deconvolution, Inverse Problems, Epigraph Sets**

I. Introduction

A wide range of deconvolution algorithms has been developed to remove blur in microscopic images in recent years [1]–[16]. In this article, two new convex sets are introduced for blind deconvolution algorithms. Both sets can be incorporated to any iterative deconvolution and/or blind deconvolution method.

One of the sets is based on the phase of the Fourier transform (FT) of the observed image. Most point spread functions blurring microscopic images are symmetric with respect to origin. Therefore, Fourier transform of such functions do not have any phase. As a result, FT phase of the original image and the blurred image have the same phase. The set of images with a prescribed phase is a closed and convex set and projection onto this convex set is easy to perform in Fourier domain.

The second set is the Epigraph Set of Total Variation (ESTV) function. Total variation (TV) value of an image can be limited by an upper-bound to stabilize the restoration process. In fact, such sets were used by many researchers in inverse problems [13], [17]–[21]. In this paper, the epigraph of the TV function will be used to automatically estimate an upper-bound on the TV value of a given image. This set is also a closed and convex set. Projection onto ESTV function can be also implemented effectively. ESTV can be incorporated into any iterative blind deconvolution algorithm.

Another contribution of this article is that the ESTV set is applied onto point spread functions (PSF) during iterative deconvolution algorithms. PSFs are smooth functions, therefore their total variation value should not be high.

Image reconstruction from Fourier transform phase information was first considered in 1980's [22]–[25] and total variation based image denoising was introduced in 1990's [26]. However, FT phase information and ESTV have not been used in blind deconvolution problem to the best of our knowledge.

Recently, Fourier phase information is used in image quality assessment and blind deblurring by Leclaire and Moisan [27], in which phase information is used to define an image sharpness index, and this index is used as a part of a deblurring algorithm. In this article FT phase is directly used during the blind deconvolution of fluorescence microscopic images.

The paper is organized as follows. In Section II, we review image reconstruction problem from FT phase and describe the convex set based on phase information. In Section III, we describe the Epigraph set of the TV function. We modify Ayers-Dainty and Richardson-Lucy blind deconvolution methods by performing orthogonal projections onto FT phase and ESTV sets in Section IV. We present our experimental results in Section V and conclude the article in Section VI.

II. Convex Set based on the phase of Fourier Transform

In this section, we introduce our notation and describe how the phase of Fourier transform can be used in deconvolution problems.

Let $x_o[n_1, n_2]$ be the original image and $h[n_1, n_2]$ be the point spread function. The observed image y is obtained by the convolution of h with x:

$$y[n_1, n_2] = h[n_1, n_2] * x_o[n_1, n_2], \tag{1}$$

where $*$ represents the two-dimensional convolution operation. Discrete-time Fourier transform Y of y is, therefore, given by

$$Y(w_1, w_2) = H(w_1, w_2) X_o(w_1, w_2). \tag{2}$$

M. Tofighi and O. Yorulmaz contributed equally and the names are listed in alphabetical order. Emails: tofighi@ee.bilkent.edu.tr, yorulmaz@ee.bilkent.edu.tr, kosek@mskcc.org, rengul@metu.edu.tr cetin@bilkent.edu.tr.

This work is funded by Turkish Scientific and Technical Research Council (TUBITAK), under project number 113E069.

When $h[n_1, n_2]$ is symmetric with respect to origin ($h[n_1, n_2] = (0, 0)$) $H(w_1, w_2)$ is real. Our zero phase assumption is $H(w_1, w_2) = |H(w_1, w_2)|$. Point spread functions satisfying this assumption includes uniform Gaussian blurs. Therefore, phase of $Y(w_1, w_2) = |Y(w_1, w_2)| \exp(j\measuredangle Y(w_1, w_2))$ and $X_o(w_1, w_2) = |X_0(w_1, w_2)|exp(j\measuredangle X_o(w_1, w_2))$ are the same:

$$\measuredangle Y(w_1, w_2) = \measuredangle X_o(w_1, w_2), \tag{3}$$

for all (w_1, w_2) values. Based on the above observation the following set can be defined:

$$C_\phi = \{x[n_1, n_2] \mid \measuredangle X(w_1, w_2) = \measuredangle X_o(w_1, w_2)\}, \tag{4}$$

which is the set of images whose FT phase is equal to a given prescribed phase $\measuredangle X_o(w_1, w_2)$.

It can easily be shown that this set is closed and convex in $\mathbb{R}^{N_1} \times \mathbb{R}^{N_2}$, for images of size $N_1 \times N_2$.

Projection of an arbitrary image x onto C_ϕ is implemented in Fourier domain. Let the FT of x be $X(w_1, w_2) = |X(w_1, w_2)|e^{j\phi(w_1, w_2)}$. The FT X_p of its projection x_p is obtained as follows:

$$X_p(w_1, w_2) = |X(w_1, w_2)|e^{j\measuredangle X_o(w_1, w_2)}, \tag{5}$$

where the magnitude of $X_p(w_1, w_2)$ is the same as the magnitude of $X(w_1, w_2)$ but its phase is replaced by the prescribed phase function $\measuredangle X_o(w_1, w_2)$. After this step, $x_p[n_1, n_2]$ is obtained using the inverse FT. The above operation is implemented using the FFT and implementation details are described in Section IV.

Obviously, projection of y onto the set C_ϕ is the same as itself. Therefore, the iterative blind deconvolution algorithm should not start with the observed image. Image reconstruction from phase (IRP) has been extensively studied by Oppenheim and his coworkers [22]–[25]. IRP problem is a robust inverse problem. In Figure 1, phase only version of the well-known Lena image is shown. The phase only image is obtained as follows:

$$v = \mathcal{F}^{-1}[Ce^{j\phi(w_1, w_2)}] \tag{6}$$

where $\mathcal{F}^{-1}$. represents the inverse Fourier transform, C is a constant and $\phi(w_1, w_2)$ is the phase of Lena image. Edges of the original image are clearly observable in the phase only image. Therefore, the set C_ϕ contains the crucial edge information of the original image x_o.

When the support of x_o is known it is possible to reconstruct the original image from its phase within a scale factor. Oppenheim and coworkers developed Papoulis-Gerchberg type iterative algorithms from a given phase information. In [24] support and phase information are imposed on iterates in space and Fourier domains in a successive manner to reconstruct an image from its phase.

In blind deconvolution problem the support regions of x_o and y are different from each other. Exact support of the original image is not precisely known; therefore, C_ϕ is not sufficient by itself to solve the blind deconvolution problem. However, it can be used as a part of any iterative blind deconvolution method.

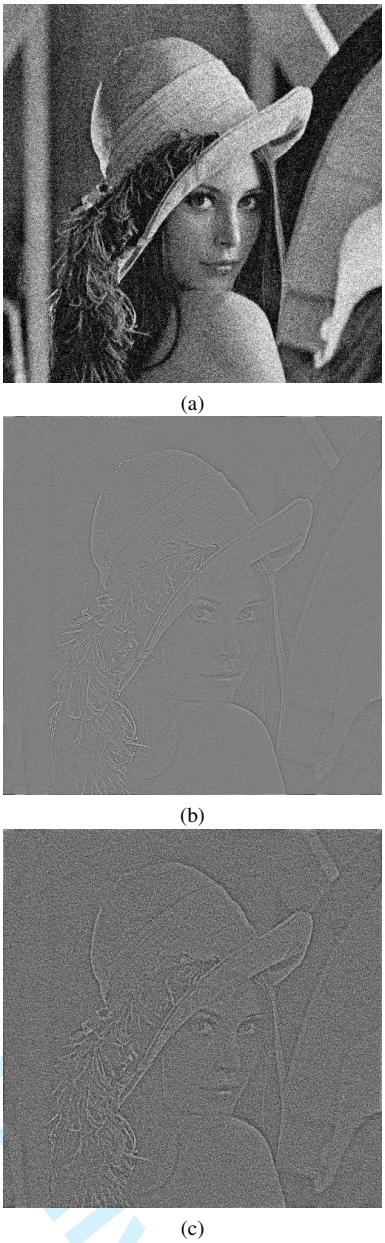

(a) (b) (c)

Fig. 1: (a) noisy "Lena" image, (b) Phase only version of the "Lena" image, and (c) phase only version of the noisy "Lena" image.

When there is observation noise, Eq. (1) becomes:

$$\mathbf{y}_o = \mathbf{y} + \boldsymbol{\nu}, \tag{7}$$

where $\boldsymbol{\nu}$ represents the additive noise. In this case, phase of the observed image is obviously different from the phase of the original image. Luckily, phase information is robust to noise as shown in Fig. 1c which is obtained from a noisy version of Lena image. In spite of noise, edges of Lena are clearly visible in the phase only image. Gaussian noise with variance $\sigma = 30$ is added to Lena image in Fig. 1a.

FTs of some symmetric point spread function may take negative values for some (w_1, w_2) values. In such (w_1, w_2) values, phase of the observed image $Y(w_1, w_2)$ differs from $X(w_1, w_2)$ by π. Therefore, phase of $Y(w_1, w_2)$ should be corrected as in phase unwrapping algorithms. Or some of the

(w_1, w_2) values around $(w_1,\ w_2) = (0,\ 0)$ can be used during the image reconstruction process. It is possible to estimate the main lobe of the FT of the point spread function from the observed image. Phase of FT coefficients within the main lobe are not effected by a shift of π.

In this article, the set C_ϕ will be used as a part of the iterative blind deconvolution schemes developed by Dainty *et al* [28] and Fish *et al* [29], together with the epigraph set of total variation function which will be introduced in the next section.

III. Epigraph Set of Total Variation Function

Bounded total variation is widely used in various image denoising and related applications [17], [18], [30]–[33]. The set C_{TV} of images whose TV values is bounded by a prescribed number ϵ is defined as follows:

$$C_{\text{TV}} = \{\mathbf{x} : \text{TV}(\mathbf{x}) \leq \epsilon\}, \tag{8}$$

where TV of an image is defined, in this paper, as follows:

$$\text{TV}(\mathbf{x}) = \sum_{i,j=1}^{N_1} |x^{i+1,j} - x^{i,j}| + \sum_{i,j=1}^{N_2} |x^{i,j+1} - x^{i,j}|. \tag{9}$$

This set is a closed and convex set in $\mathbb{R}^{N_1 \times N_2}$. Set C_{TV} can be used in blind deconvolution problems. But the upper bound ϵ has to be determined somehow a priori.

In this article we increase the dimension of the space by 1 and consider the problem in $\mathbb{R}^{N_1 \times N_2 + 1}$. We define the epigraph set of the TV function:

$$\text{C}_{ESTV} = \{\underline{\mathbf{x}} = [x^T\ z]^T \mid \text{TV}(\mathbf{x}) \leq z\}, \tag{10}$$

where T is the transpose operation and we use bold face letters for N dimensional vectors and underlined bold face letters for $N+1$ dimensional vectors, respectively.

The concept of the epigraph set is graphically illustrated in Fig. 2. Since $\text{TV}(\mathbf{x})$ is a convex function in $\mathbb{R}^{N_1 \times N_2}$ set the C_{ESTV} is closed and convex in $\mathbb{R}^{N_1 \times N_2 + 1}$. In Eq. (10) one does not need to specify a prescribed upper bound on TV of an image. An orthogonal projection onto the set C_{ESTV} reduces the total variation value of the image as graphically illustrated in Fig. 2 because of the convex nature of the TV function. Let $\mathbf{v}$ be an $N = N_1 \times N_2$ dimensional image to be projected onto the set C_{ESTV}. In orthogonal projection operation, we select the nearest vector $\underline{\mathbf{x}}^\star$ on the set C_{ESTV} to $\underline{\mathbf{w}}$. The projection vector $\mathbf{x}^\star$ of an image $\mathbf{v}$ is defined as:

$$\underline{\mathbf{w}}^\star = \arg \min_{\underline{\mathbf{w}} \in C_{\text{ESTV}}} \|\underline{\mathbf{v}} - \underline{\mathbf{w}}\|^2, \tag{11}$$

where $\underline{\mathbf{v}}$ = $[\mathbf{v}^T\ 0]$. The projection operation described in (11) is equivalent to:

$$\underline{\mathbf{w}}^\star = \begin{bmatrix} \mathbf{w}_p \\ \text{TV}(\mathbf{w}_p) \end{bmatrix} = \arg \min_{\underline{\mathbf{w}} \in \text{C}_\text{f}} \| \begin{bmatrix} \mathbf{v} \\ 0 \end{bmatrix} - \begin{bmatrix} \mathbf{w} \\ \text{TV}(\mathbf{w}) \end{bmatrix} \|, \tag{12}$$

where $\underline{\mathbf{w}}^\star = [\mathbf{w}_p^T, \text{TV}(\mathbf{w}_p)]$ is the projection of $(\mathbf{v}, 0)$ onto the epigraph set. The projection $\underline{\mathbf{w}}^\star$ must be on the boundary of the epigraph set. Therefore, the projection must be on the form $[\mathbf{w}_p^T, \text{TV}(\mathbf{w}_p)]$. Equation (12) becomes:

$$\underline{\mathbf{w}}^\star = \begin{bmatrix} \mathbf{w}_p \\ \text{TV}(\mathbf{w}_p) \end{bmatrix} = \arg \min_{\underline{\mathbf{w}} \in \text{C}_\text{f}} \|\mathbf{v} - \mathbf{w}\|_2^2 + \text{TV}(\mathbf{w})^2. \tag{13}$$

It is also possible to use $\lambda\text{TV}(.)$ as the convex cost function and Eq. 13 becomes:

$$\underline{\mathbf{w}}^\star = \begin{bmatrix} \mathbf{w}_p \\ \text{TV}(\mathbf{w}_p) \end{bmatrix} = \arg \min_{\underline{\mathbf{w}} \in \text{C}_\text{f}} \|\mathbf{v} - \mathbf{w}\|_2^2 + \lambda^2 \text{TV}(\mathbf{w})^2. \tag{14}$$

The solution of (11) can be obtained using the method that we discussed in [32], [34]. The solution is obtained in an iterative manner and the key step in each iteration is an orthogonal projection onto a supporting hyperplane of the set C_{ESTV}.

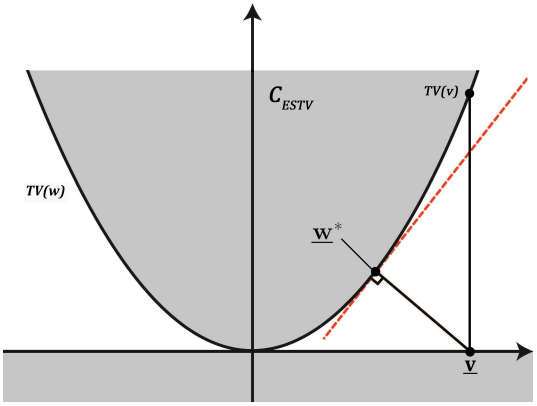

Fig. 2: Graphical representation of the orthogonal projection onto the set C_{ESTV} defined in (11). The observation vector $\underline{\mathbf{v}} = [v^T\ 0]^T$ is projected onto the set C_{ESTV}, which is the epigraph set of TV function

In current TV based denoising methods [18], [31] the following cost function is used:

$$\min \|\mathbf{v} - \mathbf{w}\|_2^2 + \lambda \text{TV}(\mathbf{w}). \tag{15}$$

However, we were not able to prove that 15 corresponds to a non-expansive map or not. On the other hand, minimization problem in Eq. (13) and (14) are the results of projection onto convex sets, as a result they correspond to non-expansive maps [5], [17], [30], [35], [35]–[41]. Therefore, they can be incorporated into any iterative deblurring algorithm without affecting the convergence of the algorithm.

IV. How to incorporate C_{ESTV} and C_ϕ into a deblurring method

In this section, we present our implementation to integrate phase and TV based convex sets approach into two well known blind deconvolution algorithms.

A. Blind Ayers-Dainty Method with Phase and ESTV sets

One of the earliest blind deconvolution methods is the iterative space-Fourier domain method developed by Ayers and Dainty [28]. In this approach, iterations start with a $x_o[n] = x_o[n_1, n_2]$, where we introduce a new notation to specify equations $[n] = [n_1, n_2]$. For example, we rewrite Eq. (1) as follows:

$$y[n] = h[n] * x_o[n]. \tag{16}$$

The method successively updates $h[n]$ and $x[n]$ in a Wiener filter-like equation. Here is the i^{th} step of the algorithm:

1) Compute $\hat{X}_i(w) = \mathcal{F}\{x_i[n]\}$, where $\mathcal{F}$ represents the FT operation and $w = (w_1, w_2)$, with some abuse of notation.
2) Estimate the point-spread filter response using the following equation

$$\tilde{H}_i(w) = \frac{Y(w)\hat{X}_i^*(w)}{|\hat{X}_i(w)|^2 + \alpha/|\hat{H}_i(w)|^2}, \quad (17)$$

where α is a small real number.
3) Compute $\tilde{h}_i[n] = \mathcal{F}^{-1}\{\tilde{H}_i(w)\}$
4) Impose the positivity constraint and finite support constraints on $\tilde{h}_i[n]$. Let the output of this step be $\hat{h}_i[n]$.
5) Compute $\hat{H}_i(w) = \mathcal{F}\{\hat{h}_i[n]\}$
6) Update the image

$$\tilde{X}_i(w) = \frac{Y(w)\hat{H}_i^*(w)}{|\hat{H}_i(w)|^2 + \alpha/|\hat{X}_i(w)|^2}, \quad (18)$$

7) Compute $\hat{x}_i[n] = \mathcal{F}^{-1}\{\hat{X}_i(w)\}$
8) Impose spatial domain positivity and finite support constraint on $\hat{x}_i[n]$ to produce the next iterate $\hat{x}_{i+1}[n]$.

Iterations are stopped when there is no significant change between successive iterates. We can easily modify this algorithm using the convex sets defined in Section II and III. We introduce another step after step 6 as follows:

Impose the phase information

$$\bar{X}_i(w) = |\tilde{X}_i(w)|e^{j\measuredangle Y(w)}, \quad (19)$$

where $\measuredangle Y(w)$ is the phase of $Y(w)$. This step is the projection onto the set C_ϕ. As a result step 7 becomes $\tilde{x}_i[n] = \mathcal{F}^{-1}\{\bar{X}_i(w)\}$. We also introduce a new step to Ayers and Dainty's algorithm as follows: Project $\tilde{x}_i[n]$ onto the set C_{ESTV} to obtain $\hat{x}_{i+1}[n]$. The flowchart of the proposed algorithm is shown in Fig. 3.

Since the filter is a zero-phase filter in microscopic image analysis $h[n_1, n_2] = h[-n_1, -n_2] = h[-n_1, n_2] = h[n_1, -n_2]$ this condition is also imposed on the current iterate in Step 4.

Global convergence of Ayers-Dainty method has not been proved. In fact, we experimentally observed that it may diverge in some FL microscopy images. Projections onto convex sets are non-expansive maps [41]–[43], therefore, they do not cause any divergence problems in an iterative image debluring algorithm.

B. Lucy-Richardson Based Blind Deconvolution Method with Phase and ESTV sets

A well known deconvolution method is proposed in 1972 and 1974 by Richardson [44] and Lucy [45]. Method which is also known as Richardson–Lucy Algorithm makes use of Bayes's theorem to iteratively recover an image that is filtered with a known PSF. Noise resistant algorithm is improved and used in many optics and medical imaging applications [46].

In Richardson-Lucy method, at *i*'th iteration, image estimate $\tilde{x}[n]$ is found as follows:

$$\tilde{x}_{i+1}[n] = \left(\left(\frac{y[n]}{\tilde{x}_i[n] * h[n]}\right) * h[-n]\right)\tilde{x}_i[n] \quad (20)$$

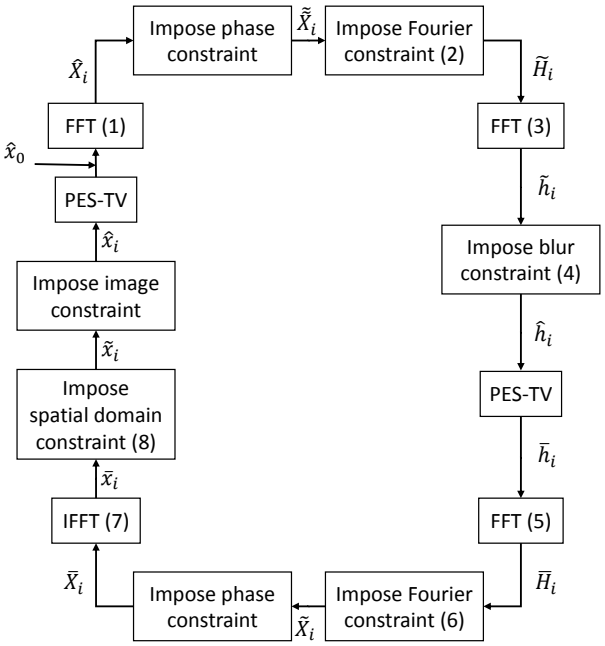

Fig. 3: Flowchart of the proposed algorithm on Ayers-Dainty method. PES-TV stands for Projection onto the Epigraph Set of TV function.

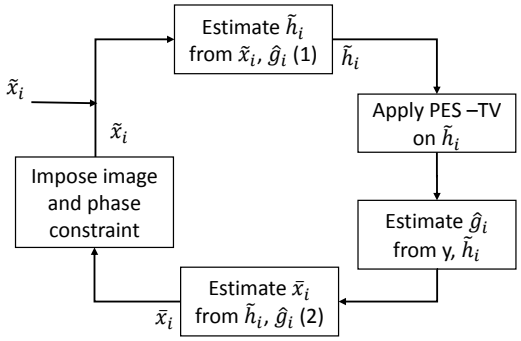

Fig. 4: Flowchart of the proposed algorithm on blind Richardson-Lucy method. PES-TV stands for Projection onto the Epigraph Set of TV function.

where $\tilde{x}_i[n]$ is the estimate of $x[n]$ in *i*'th iteration, $y[n]$ is the convolution of $x[n]$ and $h[n]$. In [29], the algorithm is modified as a blind deconvolution method which estimates the PSF of filter and the image from each other in an iterative manner. The steps of this algorithm in *i*'th iteration are given as follows:

1) Estimate the point-spread filter response $\tilde{h}_{i+1}[k]$ using:

$$\tilde{h}_{i+1}[n] = \left(\left(\frac{y[n]}{\tilde{x}_i[n] * \tilde{h}_i[n]}\right) * \tilde{h}_i[-n]\right)\tilde{x}_i[n] \quad (21)$$

iteratively.
2) Estimate the image $\tilde{x}_{i+1}[k]$ using:

$$\tilde{x}_{i+1}[n] = \left(\left(\frac{y[n]}{\tilde{x}_i[n] * \tilde{h}_i[n]}\right) * \tilde{x}_i[-n]\right)\tilde{h}_i[n] \quad (22)$$

iteratively.

In order to use phase information, we initially assumed that a wide black border exists around the image. PSF extends the original image $x[n]$ into the dark region because of the convolution operation. An image $\hat{g}_i[n]$ is defined at each iteration from the observed image and the estimated filter $\tilde{h}_i$ as follows:

$$\hat{g}_i[n] = \begin{cases} y[n], & n \in I \\ y[n] * \tilde{h}_i[n], & n \notin I \end{cases} \quad (23)$$

where I represents the support of the observed and actual image. The image $\hat{g}_i[n]$ occupies a larger area and its extent is determined by the filter $\hat{h}_i[n]$.

In each iteration between (21) and (22), PES-TV is applied to the filter estimate $\tilde{h}_i$. To correct the phase of $\tilde{x}_i[n]$ we perform the following operation:

$$\tilde{X}_i(w) = |\bar{X}_i(w)| e^{j \angle \hat{G}_i(w)}, \quad (24)$$

The phase of the image $\bar{x}_i$ is corrected using the phase of $\hat{g}_i$ instead of the phase of y because the phase of $\hat{g}_i$ should be closer to the phase of the original image x.

The flowchart of the proposed algorithm is given in Figure 4. Projections onto FT phase and ESTV sets can be incorporated to other deconvolution methods such as [47].

TV regularization is considered in Richardson-Lucy's method in [14]. However, we not only apply the TV regularization onto images but also to the PSF of the filter because PSF coefficients should not have high TV values in practice.

V. Experimental Results

The proposed algorithm is evaluated using different fluorescence (FL) microscopy images obtained at Bilkent University as a part of a project funded by Turkish Scientific Research Council and German BMBF to track the motility and migration of cells. The contact inhibition phenomena as a result of cell migration was first described in 1950s [48] in cultured cells which indicated that cell migration and motility are under the control of cell signaling. Cell migration and motility is a cellular activity that occurs during various stages of the life cycle of a cell under normal or pathological conditions. Embryonic development, wound-tissue healing, inflammation, angiogenesis, cancer metastasis are some of the major cellular activities that involve cell motility.

We used a video object tracker to track cells in our research. But the performance was very poor because the FL cell images were very smooth. Therefore we decided to develop a blind deconvolution method to obtain sharp cell images. After blind deconvolution, cells have clear features and sharper edges which can be used by video object trackers to track the motility of individual cells.

In order to evaluate PSNR we selected relatively sharp cell images from FL images and we synthetically blurred them using a 20×20 Gaussian filter with $\sigma = 5$. We also visually checked the results of our algorithm on naturally blurred images. We tested proposed method against blind Ayers-Dainty [28] and blind Richardson-Lucy methods [29] to observe the improvement. In Ayers-Dainty based methods, we started by an impulse image in which only one component was nonzero, as the initial guess. This way we ensured that all the frequency components would have a nonzero magnitude value. In Richardson-Lucy based methods, the initial guess was the blurry image itself. Furthermore we compared our method with another blind deconvolution method proposed in [16], which achieve deblurring by minimizing a regularization cost.

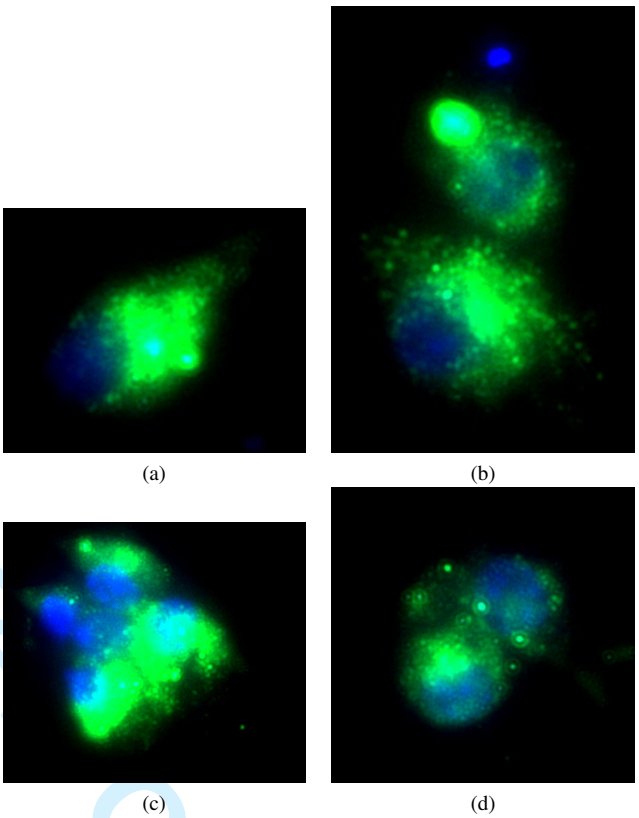

Fig. 5: Sample fluorescence microscopic images used in experiments (a) Im-1, (b) Im-2 (c) Im-3, and (d) Im-4.

In Fig 5, sample images are shown that are used in experimental studies. For Ayers-Dainty and Richardson-Lucy methods, we compared each algorithm with their own extensions using FT phase and ESTV. In blind Richardson-Lucy implementation we have two types of iterations. We limited the number of iterations by 30 and inner iterations described in Equations (21) and (22) by 40. We stopped if the estimation difference of consecutive iterations became smaller than a given threshold. Phase and ESTV sets clearly improved the blind Richardson-Lucy method as shown in Table I.

For Ayers-Dainty methods, we limited the number of iterations to 300 and stopped if the estimation difference of consecutive iterations became smaller than a prescribed threshold. We tested the cases with Ayers-Dainty [28], Ayers-Dainty and ESTV, Ayers-Dainty and Phase, and the proposed Ayers-Dainty with Phase and ESTV sets. The comparison of the PSNR performances of these algorithms is given in Table II.

We also used blind deconvolution method proposed in [16] to deblur FL microscopy images as shown in Table II. The PSNR performance of this algorithm is not as good as the

TABLE I: Deconvolution results for FL microscopic images blurred by a Gaussian filter with filter size 20×20 and $\sigma = 5$. PSNR (dB) values are reported.

Image	Blind Richardson-Lucy	Blind Richardson-Lucy with Phase and ESTV sets
im-1	17.91	**30.05**
im-2	25.83	**28.97**
im-3	23.07	**25.25**
im-4	19.36	**26.71**
im-5	21.99	**26.66**
im-6	19.39	**26.09**
im-7	26.91	**27.89**
im-8	19.87	**26.28**
im-9	21.14	**26.13**
im-10	19.29	**24.93**
im-11	17.77	**26.24**
im-12	16.71	**24.50**
im-13	19.25	**26.10**
im-14	17.08	**25.95**

Ayers-Dainty method. Image deblurring results for "im-7" is shown in Figure 6.

The bold PSNR values are the best results for a given image. We observed that best blind deconvolution results are obtained with Ayers-Dainty method using phase and ESTV set in general in our FL image test set. Richardson-Lucy algorithm and the method described in [16] cannot improve fine details of FL images as shown in Figure 6 and Table II. In the following web-page you may find the MATLAB code of projections onto C_ϕ and C_{ESTV} and example FL images which four of them are shown in Fig. 5. Web-page: http://signal.ee.bilkent.edu.tr/BlindDeconvolution.html.

TABLE II: Deconvolution results for FL microscopic images blurred by a Gaussian filter with disc size 20 and $\sigma = 5$. PSNR (dB) values are reported.

Image	Ayers-Dainty	Ayers-Dainty with Phase	Ayers Dainty with ESTV	Ayers Dainty Phase&ESTV	Method in [16]
im-1	30.85	31.10	30.99	**31.34**	29.36
im-2	35.93	35.11	**36.56**	36.39	29.68
im-3	32.63	33.32	32.76	**33.53**	28.92
im-4	30.48	34.99	32.27	**36.79**	29.88
im-5	35.77	35.79	36.22	**36.37**	28.24
im-6	33.74	35.38	33.91	**35.53**	29.33
im-7	31.29	31.57	**32.23**	32.03	30.77
im-8	32.59	33.25	33.39	**33.69**	29.55
im-9	30.64	**30.80**	30.07	29.38	29.01
im-10	34.68	35.74	34.93	**35.92**	28.68
im-11	36.57	36.25	**36.82**	36.52	30.61
im-12	**37.03**	35.80	37.56	36.66	30.48
im-13	37.49	37.73	38.16	**38.29**	28.81
im-14	31.73	31.40	**31.93**	31.78	30.26

VI. Conclusion

Both FT phase and the epigraph set of the TV function are closed and convex sets. They can be used as a part of iterative microscopic image deblurring algorithms. Both sets not only provide additional information about the desired solution but they also stabilize the deconvolution algorithms. It is experimentally observed that they significantly improve the blind deblurring results of Ayers and Dainty's method and Richardson-Lucy algorithms in FL microscopy images.

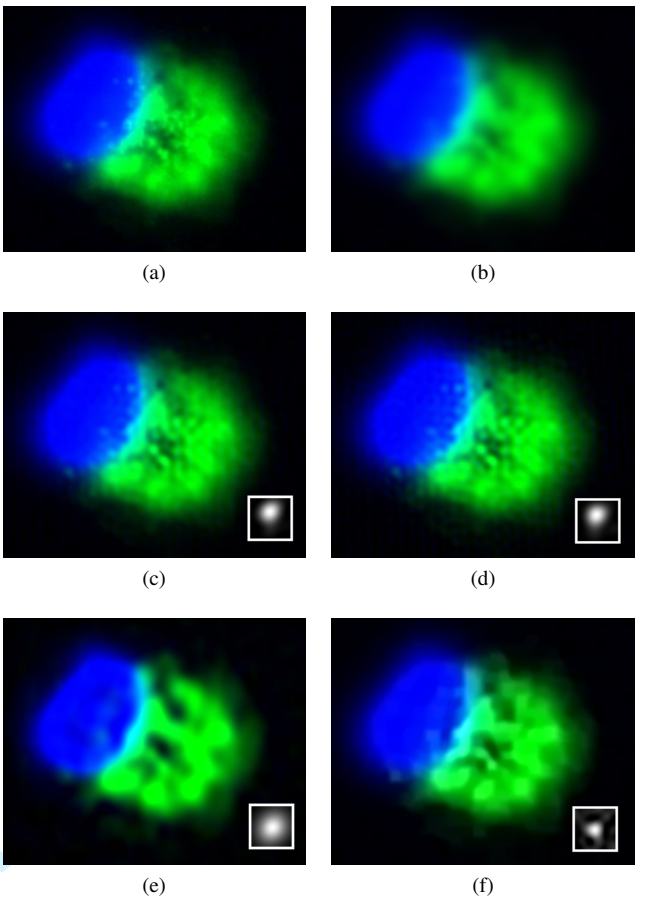

(a) (b) (c) (d) (e) (f)

Fig. 6: Sample deblurring results for "im-7": (a) Original image, (b) blurred image (Gaussian $\sigma = 5$). (c) Image obtained by Ayers-Dainty with Phase and ESTV sets, (d) Ayers-Dainty method, (e) blind Richardson-Lucy with phase and ESTV sets and (f) image obtained using [16]. PSF estimate for each case is shown in the bottom right corner.

References

[1] P. Campisi and K. Egiazarian, *Blind image deconvolution: theory and applications*. CRC press, 2007.

[2] D. Kundur and D. Hatzinakos, "Blind image deconvolution," *Signal Processing Magazine, IEEE*, vol. 13, no. 3, pp. 43–64, May 1996.

[3] T. Chan and C.-K. Wong, "Total variation blind deconvolution," *Image Processing, IEEE Transactions on*, vol. 7, no. 3, pp. 370–375, Mar 1998.

[4] M. Sezan and H. Trussell, "Prototype image constraints for set-theoretic image restoration," *Signal Processing, IEEE Transactions on*, vol. 39, no. 10, pp. 2275–2285, Oct 1991.

[5] M. Sezan, "An overview of convex projections theory and its application to image recovery problems," *Ultramicroscopy*, vol. 40, no. 1, pp. 55 – 67, 1992.

[6] H. Trussell and M. Civanlar, "The feasible solution in signal restoration," *Acoustics, Speech and Signal Processing, IEEE Transactions on*, vol. 32, no. 2, pp. 201–212, Apr 1984.

[7] L. Xu, S. Zheng, and J. Jia, "Unnatural l0 sparse representation for natural image deblurring," in *Computer Vision and Pattern Recognition (CVPR), 2013 IEEE Conference on*, June 2013, pp. 1107–1114.

[8] P. Ye, H. Feng, Q. Li, Z. Xu, and Y. Chen, "Blind deconvolution using an improved l0 sparse representation," pp. 928 419–928 419–6, 2014.

[9] J. Boulanger, C. Kervrann, and P. Bouthemy, "Adaptive spatio-temporal restoration for 4d fluorescence microscopic imaging," in *Medical Image Computing and Computer-Assisted Intervention – MICCAI 2005*, ser. Lecture Notes in Computer Science, J. Duncan and G. Gerig, Eds. Springer Berlin Heidelberg, 2005, vol. 3749, pp. 893–901.

[10] C. Sorzano, E. Ortiz, M. López, and J. Rodrigo, "Improved bayesian image denoising based on wavelets with applications to electron microscopy," *Pattern Recognition*, vol. 39, no. 6, pp. 1205 – 1213, 2006.

[11] S. Acton, "Deconvolutional speckle reducing anisotropic diffusion," in *Image Processing, 2005. ICIP 2005. IEEE International Conference on*, vol. 1, Sept 2005, pp. I–5–8.

[12] N. Dey, L. Blanc-Feraud, C. Zimmer, P. Roux, Z. Kam, J.-C. Olivo-Marin, and J. Zerubia, "Richardson–lucy algorithm with total variation regularization for 3d confocal microscope deconvolution," *Microscopy Research and Technique*, vol. 69, no. 4, pp. 260–266, 2006.

[13] N. Dey, L. Blanc-Féraud, C. Zimmer, P. Roux, Z. Kam, J.-C. Olivo-Marin, and J. Zerubia, "3D Microscopy Deconvolution using Richardson-Lucy Algorithm with Total Variation Regularization," Research Report RR-5272, 2004.

[14] P. Pankajakshan, B. Zhang, L. Blanc-Féraud, Z. Kam, J.-C. Olivo-Marin, and J. Zerubia, "Blind deconvolution for thin-layered confocal imaging," *Appl. Opt.*, vol. 48, no. 22, pp. 4437–4448, Aug 2009.

[15] B. Zhang, J. Zerubia, and J.-C. Olivo-Marin, "Gaussian approximations of fluorescence microscope point-spread function models," *Appl. Opt.*, vol. 46, no. 10, pp. 1819–1829, Apr 2007.

[16] D. Krishnan, T. Tay, and R. Fergus, "Blind deconvolution using a normalized sparsity measure," in *Computer Vision and Pattern Recognition (CVPR), 2011 IEEE Conference on*. IEEE, 2011, pp. 233–240.

[17] P. L. Combettes and J. Pesquet, "Image restoration subject to a total variation constraint," *IEEE Transactions on Image Processing*, vol. 13, pp. 1213–1222, 2004.

[18] P. L. Combettes and J.-C. Pesquet, "Proximal splitting methods in signal processing," in *Fixed-Point Algorithms for Inverse Problems in Science and Engineering*, ser. Springer Optimization and Its Applications, H. H. Bauschke, R. S. Burachik, P. L. Combettes, V. Elser, D. R. Luke, and H. Wolkowicz, Eds. Springer New York, 2011, pp. 185–212.

[19] K. Kose, V. Cevher, and A. E. Cetin, "Filtered variation method for denoising and sparse signal processing," *IEEE International Conference on Acoustics, Speech and Signal Processing (ICASSP)*, pp. 3329–3332, 2012.

[20] G. Chierchia, N. Pustelnik, J.-C. Pesquet, and B. Pesquet-Popescu, "An epigraphical convex optimization approach for multicomponent image restoration using non-local structure tensor," in *Acoustics, Speech and Signal Processing (ICASSP), 2013 IEEE International Conference on*, 2013, pp. 1359–1363.

[21] ——, "Epigraphical projection and proximal tools for solving constrained convex optimization problems," *Signal, Image and Video Processing*, pp. 1–13, 2014.

[22] M. Hayes, J. Lim, and A. Oppenheim, "Signal reconstruction from phase or magnitude," *Acoustics, Speech and Signal Processing, IEEE Transactions on*, vol. 28, no. 6, pp. 672–680, Dec 1980.

[23] A. Oppenheim and J. Lim, "The importance of phase in signals," *Proceedings of the IEEE*, vol. 69, no. 5, pp. 529–541, May 1981.

[24] A. V. Oppenheim, M. H. Hayes, and J. S. Lim, "Iterative procedures for signal reconstruction from fourier transform phase," *Optical Engineering*, vol. 21, no. 1, pp. 211 122–211 122–, 1982.

[25] S. Curtis, J. Lim, and A. Oppenheim, "Signal reconstruction from one bit of fourier transform phase," in *Acoustics, Speech, and Signal Processing, IEEE International Conference on ICASSP '84.*, vol. 9, Mar 1984, pp. 487–490.

[26] L. I. Rudin, S. Osher, and E. Fatemi, "Nonlinear total variation based noise removal algorithms," *Physica D: Nonlinear Phenomena*, vol. 60, no. 1–4, pp. 259 – 268, 1992.

[27] A. Leclaire and L. Moisan, "No-reference image quality assessment and blind deblurring with sharpness metrics exploiting fourier phase information," *Journal of Mathematical Imaging and Vision*, vol. 52, no. 1, pp. 145–172, 2015.

[28] G. R. Ayers and J. C. Dainty, "Iterative blind deconvolution method and its applications," *Opt. Lett.*, vol. 13, no. 7, pp. 547–549, Jul 1988.

[29] D. Fish, J. Walker, A. Brinicombe, and E. Pike, "Blind deconvolution by means of the richardson–lucy algorithm," *JOSA A*, vol. 12, no. 1, pp. 58–65, 1995.

[30] N. Pustelnik, C. Chaux, and J. Pesquet, "Parallel proximal algorithm for image restoration using hybrid regularization," *IEEE Transactions on Image Processing*, vol. 20, no. 9, pp. 2450–2462, 2011.

[31] A. Chambolle, "An algorithm for total variation minimization and applications," *Journal of Mathematical Imaging and Vision*, vol. 20, no. 1-2, pp. 89–97, Jan. 2004.

[32] M. Tofighi, K. Kose, and A. E. Cetin, "Denoising using projections onto the epigraph set of convex cost functions," in *Image Processing (ICIP), 2014 IEEE International Conference on*, Oct 2014, pp. 2709–2713.

[33] Y. Censor, W. Chen, P. L. Combettes, R. Davidi, and G. Herman, "On the Effectiveness of Projection Methods for Convex Feasibility Problems with Linear Inequality Constraints," *Computational Optimization and Applications*, vol. 51, no. 3, pp. 1065–1088, 2012.

[34] A. E. Cetin, A. Bozkurt, O. Gunay, Y. H. Habiboglu, K. Kose, I. Onaran, R. A. Sevimli, and M. Tofighi, "Projections onto convex sets (pocs) based optimization by lifting," *IEEE GlobalSIP, Austin, Texas, USA*, 2013.

[35] D. Youla and H. Webb, "Image restoration by the method of convex projections: Part 1 theory," *Medical Imaging, IEEE Transactions on*, vol. 1, no. 2, pp. 81–94, 1982.

[36] A. E. Cetin and A. Tekalp, "Robust reduced update kalman filtering," *Circuits and Systems, IEEE Transactions on*, vol. 37, no. 1, pp. 155–156, Jan 1990.

[37] A. E. Çetin and R. Ansari, "Convolution-based framework for signal recovery and applications," *J. Opt. Soc. Am. A*, vol. 5, no. 8, pp. 1193–1200, Aug 1988.

[38] K. Kose and A. Cetin, "Low-pass filtering of irregularly sampled signals using a set theoretic framework [lecture notes]," *Signal Processing Magazine, IEEE*, vol. 28, no. 4, pp. 117–121, July 2011.

[39] H. Trussell and M. R. Civanlar, "The Landweber Iteration and Projection Onto Convex Set," *IEEE Transactions on Acoustics, Speech and Signal Processing*, vol. 33, no. 6, pp. 1632–1634, 1985.

[40] H. Stark, D. Cahana, and H. Webb, "Restoration of arbitrary finite-energy optical objects from limited spatial and spectral information," *J. Opt. Soc. Am.*, vol. 71, no. 6, pp. 635–642, Jun 1981.

[41] P. Combettes, "The foundations of set theoretic estimation," *Proceedings of the IEEE*, vol. 81, no. 2, pp. 182–208, Feb 1993.

[42] S. Theodoridis, K. Slavakis, and I. Yamada, "Adaptive learning in a world of projections," *Signal Processing Magazine, IEEE*, vol. 28, no. 1, pp. 97–123, Jan 2011.

[43] I. Yamada, "The hybrid steepest descent method for the variational inequality problem over the intersection of fixed point sets of nonexpansive mappings," in *Inherently Parallel Algorithms in Feasibility and Optimization and their Applications*, ser. Studies in Computational Mathematics, Y. C. Dan Butnariu and S. Reich, Eds. Elsevier, 2001, vol. 8, pp. 473 – 504.

[44] W. H. Richardson, "Bayesian-based iterative method of image restoration," *JOSA*, vol. 62, no. 1, pp. 55–59, 1972.

[45] L. B. Lucy, "An iterative technique for the rectification of observed distributions," *The astronomical journal*, vol. 79, p. 745, 1974.

[46] L. A. Shepp and Y. Vardi, "Maximum likelihood reconstruction for emission tomography," *Medical Imaging, IEEE Transactions on*, vol. 1, no. 2, pp. 113–122, 1982.

[47] A. Repetti, M. Q. Pham, L. Duval, E. Chouzenoux, and J.-C. Pesquet, "Euclid in a taxicab: Sparse blind deconvolution with smoothed regularization," *Signal Processing Letters, IEEE*, vol. 22, no. 5, pp. 539–543, 2015.

[48] M. Abercrombie and J. E. Heaysman, "Invasiveness of sarcoma cells," 1954.